available at www.sciencedirect.com

SCIENCE DIRECT®

journal homepage: www.elsevier.com/locate/biochempharm

Synthesis of microtubule-interfering halogenated noscapine analogs that perturb mitosis in cancer cells followed by cell death

Ritu Aneja [a,*], *Surya N. Vangapandu* [a], *Manu Lopus* [b], *Vijaya G. Viswesarappa* [a], *Neerupma Dhiman* [c], *Akhilesh Verma* [c], *Ramesh Chandra* [c], *Dulal Panda* [b], *Harish C. Joshi* [a]

[a] *Laboratory for Drug Discovery and Research, Department of Cell Biology, Emory University School of Medicine, 615 Michael Street, Atlanta, GA 30322, USA*

[b] *School of Biosciences and Bioengineering, Indian Institute of Technology Bombay, Mumbai, India*

[c] *BR Ambedkar Center for Biomedical Research, University of Delhi, Delhi 110007, India*

ARTICLE INFO

Article history:
Received 14 February 2006
Accepted 2 May 2006

Keywords:
Cell cycle
Mitotic arrest
Anticancer
Tubulin-binding

ABSTRACT

We have previously identified the naturally occurring non-toxic antitussive phthalideisoquinoline alkaloid, noscapine as a tubulin-binding agent that arrests mitosis and induces apoptosis. Here we present high-yield efficient synthetic methods and an evaluation of anticancer activity of halogenated noscapine analogs. Our results show that all analogs display higher tubulin-binding activity than noscapine and inhibit proliferation of human cancer cells (MCF-7, MDA-MB-231 and CEM). Surprisingly, the bromo-analog is ~40-fold more potent than noscapine in inhibiting cellular proliferation of MCF-7 cells. The ability of these analogs to inhibit cellular proliferation is mediated by cell cycle arrest at the G_2/M phase, in that all analogs except 9-iodonoscapine, caused selective mitotic arrest with a higher efficiency than noscapine followed by apoptotic cell death as shown by immunofluorescence and quantitative FACS analyses. Furthermore, our results reveal the appearance of numerous fragmented nuclei as evidenced by DAPI staining. Thus, our data indicate a great potential of these compounds for studying microtubule-mediated processes and as chemotherapeutic agents for the management of human cancers.

1. Introduction

Cellular microtubules are the major cytoskeletal components in all eukaryotic cells. Microtubules are crucial for the maintenance of cell shape, polarity, and intracellular transport of vesicles and organelles [1,2]. Moreover, during cell division, microtubules form the mitotic spindle, which is a key machinery driving the alignment of replicated chromosomes to the equatorial plane and mediating subsequent segregation of chromosomes to the two daughter cells [3]. The critical role that microtubules play in cell division makes them a very suitable target for the development of chemotherapeutic drugs against the rapidly dividing cancer cells [reviewed in 4,5]. Although the effectiveness of microtubule-targeting drugs has been validated by the extensive use of several vinca alkaloids and taxanes for the treatment of a wide variety of human cancers, their clinical success has been limited by the emergence of drug-resistance and associated toxicities such as leucocytopenias, diarrhea, alopecia, and peripheral neuropathies due to the blockage of axonal transport [6–8].

* *Corresponding author*. Tel.: +1 404 727 0445; fax: +1 404 727 6256.
E-mail address: raneja@emory.edu (R. Aneja).

0006-2952/$ – see front matter
doi:10.1016/j.bcp.2006.05.004

This has prompted an ongoing worldwide search for novel microtubule-targeting compounds that display favorable toxicity profiles, have better therapeutic indices and improved pharmacological characteristics.

Among the various antimitotic agents that perturb microtubule dynamics, noscapinoids constitute an emerging class of compounds receiving considerable attention [9–16]. A key structure for the cytotoxic activity of this class of compounds is the presence of two chiral centers forcing the two aromatic rings to be non-coplanar and in half-chair conformation [17]. The lead compound, noscapine was discovered by our laboratory as a microtubule-interfering agent that binds stoichiometrically to tubulin and alters tubulin conformation [18]. Like many other antimicrotubule agents, noscapine suppresses the dynamics of microtubule assembly and blocks cell cycle progression at mitosis, followed by apoptotic cell death in a wide variety of cancer cell types [18–21]. Noscapine inhibits the progression of murine lymphoma, melanoma, and human breast tumors implanted in nude mice with little or no toxicity to the kidney, heart, liver, bone marrow, spleen, or small intestine and does not inhibit primary humoral immune responses in mice [18,22–24]. The water solubility and feasibility for oral administration also represent valuable advantages of noscapine over many other antimicrotubule drugs [25–27]. Recently, several noscapine analogs have been reported by us and others that have much better therapeutic indices and improved pharmacological profiles [9–16].

Here we describe selective and high-yield synthetic schemes for the halogenation of noscapine and an evaluation of anticancer activity of these halogenated analogs compared to the parent compound, noscapine. Our results show that all halogenated derivatives (viz. 9-fluoronoscapine (9-F-nos); 9-chloronoscapine (9-Cl-nos); 9-bromonoscapine (9-Br-nos); 9-iodonoscapine (9-I-nos)) have a higher binding affinity for tubulin as compared to noscapine. With the exception of 9-iodonoscapine, all analogs inhibited proliferation of cancer cells more actively than noscapine. They displayed much lower IC_{50} values as compared to noscapine in the two human breast cancer cell lines (MCF-7 and MDA-MB-231) and a T-cell lymphoma line, CEM. Surprisingly, 9-Br-nos showed a ~40-fold higher cytotoxic activity ($IC_{50} = 1.0 \pm 0.2$ μM) in MCF-7 cells as compared to the parent noscapine ($IC_{50} = 39.6 \pm 2.2$ μM). The cellular proliferation of the hormone-refractory MDA-MB-231 cells was inhibited by 9-Br-nos with an IC_{50} that is ~10–12-fold lower ($IC_{50} = 3.3 \pm 0.4$ μM) than that of noscapine ($IC_{50} = 36.3 \pm 1.8$ μM). This inhibition of cellular proliferation was also accompanied by the appearance of numerous fragmented nuclei at 72 h of drug exposure as shown by 4′-6-diamidino-2-phenylindole (DAPI) staining. The precise mechanism of action of these compounds involved a selective arrest of cell cycle progression at the G_2/M phase in rapidly dividing cancer cells. Interestingly, whereas noscapine-arrested cells have nearly normal bipolar spindles [12], cells arrested by all halogenated analogs of noscapine formed pronounced multipolar spindles as revealed by immunofluorescence microscopy.

2. Materials and methods

2.1. Synthesis of halogenated noscapine analogs

^{1}H NMR and ^{13}C NMR spectra were measured by 400 NMR spectrometer in a $CDCl_3$ solution and analyzed by INOVA. Proton NMR spectra were recorded at 400 MHz and were referenced with residual chloroform (7.27 ppm). Carbon NMR spectra were recorded at 100 MHz and were referenced with 77.27 ppm resonance of residual chloroform. Abbreviations for signal coupling are as follows: s, singlet; d, doublet; t, triplet; q, quartet; m, multiplet. Infrared spectra were recorded on sodium chloride discs on Mattson Genesis II FT-IR. High resolution mass spectra were collected on Thermo Finnigan LTQ-FT Hybrid mass spectrophotometer using 3-nitrobenzyl alcohol or with addition of LiI as a matrix. Melting points were determined using a Thomas-Hoover melting point apparatus and were uncorrected. All reactions were conducted with oven-dried (125 °C) reaction vessels in dry argon. All common reagents and solvents were obtained from Aldrich and were dried using 4 Å molecular sieves. The reactions were monitored by thin layer chromatography (TLC) using silica gel 60 F254 (Merck) on precoated aluminum sheets. Flash chromatography was carried out on standard grade silica gel (230–400 mesh). HPLC purity data in two different solvent systems and the peak attributions were measured in Ultimate Plus, LC Packings, Dionex, using C_{18} column as shown in Table 1.

2.2. (S)-3-((R)-9-Bromo-4-methoxy-6-methyl-5,6,7,8-tetrahydro-[1,3]dioxolo[4,5-g]isoquino-lin-5-yl)-6,7-dimethoxyisobenzofuran-1(3H)-one (2)

To a flask containing noscapine (20 g, 48.4 mmol) was added minimum amount of 48% hydrobromic acid solution (~40 ml) to dissolve or make a suspension of the reactant. To the

Table 1 – HPLC purity for halogenated analogs as determined by using two different methods

Compound	Method 1		Method 2	
	Retention time (min)	HPLC purity (%)	Retention time (min)	HPLC purity (%)
Nos	14.29	97.0	14.52	97.0
9-F-nos	15.02	97.5	15.21	97.0
9-Cl-nos	15.55	99.0	15.90	99.0
9-Br-nos	15.27	98.5	16.67	98.0
9-I-nos	16.75	97.5	16.99	97.0

In method 1, the solvent systems used were 0.1% formic acid and acetonitrile, whereas, method 2 used 0.1% formic acid and methanol. The peak attributions are indicated as retention times in minutes.

reaction mixture was added freshly prepared bromine water (~250 ml) drop wise until an orange precipitate appeared. The reaction mixture was then stirred at room temperature for 1 h to attain completion, adjusted to pH 10 using ammonia solution to afford solid precipitate. The solid precipitate was recrystallized with ethanol to afford bromo-substituted noscapine. Yield: 82%; mp 169–170 °C; IR: 2945 (m), 2800 (m), 1759 (s), 1612 (m), 1500 (s), 1443 (s), 1263 (s), 1091 (s), 933 (w) cm^{-1}; ^1H NMR ($CDCl_3$, 400 MHz), δ 7.04 (d, 1H, J = 7 Hz), 6.32 (d, 1H, J = 7 Hz), 6.03 (s, 2H), 5.51(d, 1H, J = 4 Hz), 4.55 (d, 1H, J = 4 Hz), 4.10 (s, 3H), 3.98 (s, 3H), 3.89 (s, 3H), 2.52 (s, 3H), 2.8–1.93 (m, 4H); ^{13}C NMR ($CDCl_3$, 100 MHz), δ 167.5, 151.2, 150.5, 150.1, 148.3, 140.0, 135.8, 130.8, 120.3, 120.4, 120.1, 105.3, 100.9, 100.1, 87.8, 64.4, 56.1, 56.0, 55.8, 51.7, 41.2, 27.8; MS (FAB): m/z (relative abundance, %), 494 (93.8), 492 (100), 300 (30.5), 298 (35.4); MALDI: m/z 491.37 (M^+), 493.34; ESI/tandem mass spectrometry: parent ion masses, 494, 492; daughter ion masses (intensity, %), 433 (51), 431 (37), 300 (100), 298 (93.3); HRMS (ESI): m/z Calcd. for $C_{22}H_{23}BrNO_7$ (M + 1), 493.3211; Found, 493.3215 (M + 1).

2.3. *(S)-3-((R)-9-Fluoro-4-methoxy-6-methyl-5,6,7,8-tetrahydro-[1,3]dioxolo[4,5-g]isoquino-lin-5-yl)-6,7-dimethoxyisobenzofuran-1(3H)-one (3)*

To a solution of bromonoscapine (1 g, 2.42 mmol) in anhydrous THF (20 ml) was added an excess of Amberlyst-A 26 (fluorine, polymer-supported, 2.5 g, 10 mequiv. of dry resin, the average capacity of the resin is 4 mequiv./g) and the reaction mixture refluxed for 12 h. The resin was filtered off and the solvent removed to afford the crude product which was purified by flash column chromatography (ethyl acetate/hexane = 4:1) to afford (*S*)-3-((*R*)-9-fluoro-4-methoxy-6-methyl-5,6,7,8-tetrahydro-[1,3]dioxolo[4,5-*g*]isoquinolin-5-yl)-6,7-dimethoxy-isobenzo-furan-1(3*H*)-one (**3**) as a light brown crystals. The recovery of resin was achieved by washing with 1 M NaOH and then rinsing thoroughly with water until neutrality to afford hydroxy-form of resin. It was then stirred overnight with 1 M aqueous hydrofluoric acid (250 ml), washed with acetone, ether and dried in a vacuum oven at 50 °C for 12 h to afford the regenerated Amberlyst-A 26 (fluorine, polymer-supported). Yield: 74%, light brown crystals; mp 170.8–171.1 °C; ^1H NMR ($CDCl_3$, 400 MHz): δ 7.11 (d, 1H, J = 8.0 Hz), 6.99 (d, 1H, J = 8.0 Hz), 5.44 (s, 2H), 5.21 (d, 1H, J = 4.1 Hz), 4.02 (d, 1H, J = 4.1 Hz), 3.95 (s, 3H), 3.78 (s, 3H), 3.64 (s, 3H), 2.65–2.62 (m, 2H), 2.51–2.47 (m, 2H), 2.30 (s, 3H); ^{13}C NMR ($CDCl_3$, 100 MHz): δ 167.5, 152.9, 148.4, 139.8, 134.5, 126.0, 121.8, 119.0, 108.8, 103.1, 93.8, 81.9, 64.8, 61.1, 59.7, 57.7, 55.0, 46.4, 45.8, 39.4, 20.7, 19.1; HRMS (ESI): m/z Calcd. for $C_{22}H_{23}FNO_7$ (M + 1), 432.4192; Found, 432.4196 (M + 1).

2.4. *(S)-3-((R)-9-Chloro-4-methoxy-6-methyl-5,6,7,8-tetrahydro-[1,3]dioxolo[4,5-g]iso-quinolin-5-yl)-6,7-dimethoxyisobenzofuran-1(3H)-one (4)*

To a stirred solution of noscapine (5 g, 12.01 mmol) in chloroform (200 ml), a solution of sulfuryl chloride (4.897 g, 36.28 mmol) in 100 ml chloroform was added drop wise over a period of 1 h at 5–10 °C. The reaction mixture was allowed to attain room temperature and stirring was continued for 10 h. The reaction progress was monitored using thin layer chromatography (7% methanol in chloroform). The reaction mixture was poured into 300 ml of water and extracted with chloroform (2× 200 ml). The organic layer was washed with brine, dried over anhydrous magnesium sulfate and the solvent evaporated in vacuo to afford the crude product. Purification of the crude product using flash chromatography (silica gel, 230–400 mesh) with 7% methanol in chloroform as an eluent afforded the desired product, (*S*)-3-((*R*)-9-chloro-4-methoxy-6-methyl-5,6,7,8-tetrahydro-[1,3]dioxolo[4,5-*g*]iso-quinolin-5-yl)-6,7-dimethoxyisobenzofuran-1(3*H*)-one (**4**). Yield: 90% (4.49 g), colorless needles; mp 169.0–169.1 °C; ^1H NMR ($CDCl_3$, 400 MHz): δ 7.14 (d, 1H, J = 8.26 Hz), 6.41 (d, 1H, J = 8.26 Hz), 5.93 (s, 2H), 5.27 (d, 1H, J = 4.31 Hz), 4.20 (d, 1H, J = 4.32 Hz), 3.99 (s, 3H), 3.87 (s, 3H), 3.83 (s, 3H), 2.79–2.65 (m, 2H), 2.54–2.46 (m, 2H), 2.35 (s, 3H); ^{13}C NMR ($CDCl_3$, 100 MHz): δ 167.7, 152.4, 147.5, 139.3, 134.9, 126.1, 120.3, 118.4, 108.5, 102.3, 93.5, 81.9, 64.2, 61.8, 59.6, 57.7, 54.9, 46.1, 45.2, 39.8, 20.6, 18.6; HRMS (ESI): m/z Calcd. for $C_{22}H_{23}ClNO_7$ (M + 1), 448.11481; Found, 448.11482 (M + 1).

2.5. *(S)-3-((R)-9-Iodo-4-methoxy-6-methyl-5,6,7,8-tetrahydro-[1,3]dioxolo[4,5-g]isoquino-lin-5-yl)-6,7-dimethoxyisobenzofuran-1(3H)-one (5)*

The iodination of noscapine was achieved using pyridine–iodine chloride. Since this is not commercially available, we first prepared the said reagent using the following procedure. Iodine chloride (55 ml, 1 mol) was added to a solution of potassium chloride (120 g, 1.6 mol) in water (350 ml). The volume was then adjusted to 500 ml to give a 2 M solution. In the event the iodine chloride was under or over chlorinated, the solution was either filtered or the calculated quantity of potassium iodide added. Over chlorination was more to be avoided than under chlorination since iodine trichloride can serve as a chlorinating agent. Alternatively, the solution of potassium iododichloride was made as follows. A mixture of potassium iodate (71 g, 0.33 mol), potassium chloride (40 g, 0.53 mol) and conc. hydrochloric acid (5 ml) in water (80 ml) was stirred vigorously and treated simultaneously with potassium iodide (111 g, 0.66 mol) in water (100 ml) and with conc. hydrochloric acid (170 ml). The rate of addition of hydrochloric acid and potassium iodide solutions were regulated such that no chlorine was evolved. After addition was completed, the volume was brought to 500 ml with water to give a 2N solution of potassium iododichloride, which itself is a very good iodinating agent. However, usage of reagent in the aromatic iodination of noscapine resulted in hydrolysis products due to the acidic nature of the reagent. This prompted us to make basic iodinating reagent, pyridine–iodine chloride and was prepared as follows. To a stirred solution of pyridine (45 ml) in water (1 l) was added 2 M solution of potassium iododichloride (250 ml). A cream colored solid separated, the pH of the mixture was adjusted to 5.0 with pyridine and the solid collected by filtration, washed with water and air-dried to afford the pyridine–iodine chloride reagent in 97.5% yield (117 g) that was crystallized from benzene to afford light yellow solid.

Iodination of noscapine was now carried out by addition of pyridine–iodine chloride (1.46 g, 6 mmol) to a solution of

noscapine (1 g, 2.42 mmol) in acetonitrile (20 ml) and the resultant mixture was stirred at room temperature for 6 h and then at 100 °C for 6 h. After cooling, excess ammonia was added and filtered through celite pad to remove the black nitrogen triiodide. The filtrate was made acidic with 1 M HCl and filtered to collect the yellow solid, washed with water and air-dried to afford (*S*)-3-((*R*)-9-iodo-4-methoxy-6-methyl-5,6,7,8-tetrahydro-[1,3]dioxolo[4,5-*g*]isoquinolin-5-yl)-6,7-dimethoxyisobenzofuran-1(3*H*)-one (5). Yield: 76%, mp 172.3–172.6 °C; ^{1}H NMR ($CDCl_3$, 400 MHz): δ 7.15 (d, 1H, J = 8.1 Hz), 7.01 (d, 1H, J = 8.1 Hz), 6.11 (s, 2H), 5.36 (d, 1H, J = 4.8 Hz), 4.25 (d, 1H, J = 4.8 Hz), 3.85 (s, 3H), 3.74 (s, 3H), 3.72 (s, 3H), 2.78–2.72 (m, 2H), 2.55–2.50 (m, 2H), 2.32 (s, 3H); ^{13}C NMR ($CDCl_3$, 100 MHz): δ 168.2, 155.1, 151.5, 148.3, 146.5, 143.1, 140.3, 120.4, 119.5, 113.3, 101.5, 85.9, 82.2, 61.8, 56.6, 55.7, 54.5, 54.1, 51.2, 39.8, 30.1, 18.8; HRMS (ESI): *m*/*z* Calcd. for $C_{22}H_{23}INO_7$ (M + 1), 540.3209; Found, 540.3227 (M + 1).

2.6. HPLC purity and peak attributions

2.6.1. Method 1

Ultimate Plus, LC Packings, Dionex, C_{18} column (pep Map 100, 3 μm, 100 Å particle size, i.d.: 1000 μm, length: 15 cm) with solvent systems A (0.1% formic acid in water) and B (acetonitrile), a gradient starting from 100% A and 0% B to 0% A and 100% B over 25 min at a flow of 40 μl/min (Table 1).

2.6.2. Method 2

Ultimate Plus, LC Packings, Dionex, C_{18} column (pep Map 100, 3 μm, 100 Å particle size, i.d.: 1000 μm, length: 15 cm) with solvent systems A (0.1% formic acid in water) and B (methanol), a gradient starting from 100% A and 0% B to 0% A and 100% B over 25 min at a flow of 40 μl/min (Table 1).

2.6.3. Cell lines and chemicals

Cell culture reagents were obtained from Mediatech, Cellgro. CEM, a human lymphoblastoid line was provided by Dr. William T. Beck (Cancer Center, University of Illinois at Chicago). MCF-7 cells were maintained in Dulbecco's Modification of Eagle's Medium 1× (DMEM) with 4.5 g/l glucose and L-glutamine (Mediatech, Cellgro) supplemented with 10% fetal bovine serum (Invitrogen, Carlsbad, CA) and 1% penicillin/streptomycin (Mediatech, Cellgro). MDA-MB-231 and CEM cells were grown in RPMI-1640 medium supplemented with 10% fetal bovine serum, and 1% penicillin/streptomycin. Mammalian brain microtubule proteins were isolated by two cycles of polymerization and depolymerization and tubulin was separated from the microtubule binding proteins by phosphocellulose chromatography. The tubulin solution was stored at −80 °C until use.

2.7. In vitro cell proliferation assays

2.7.1. Sulforhodamine B (SRB) assay

The cell proliferation assay was performed in 96-well plates as described previously [12,28]. Adherent cells (MCF-7 and MDA-MB-231) were seeded in 96-well plates at a density of 5×10^3 cells per well. They were treated with increasing concentrations of the halogenated analogs the next day while in log-phase growth. After 72 h of drug treatment, cells were fixed with 50% trichloroacetic acid and stained with 0.4% sulforhodamine B dissolved in 1% acetic acid. After 30 min, cells were then washed with 1% acetic acid to remove the unbound dye. The protein-bound dye was extracted with 10 mM Tris base to determine the optical density at 564-nm wavelength.

2.7.2. MTS assay

Suspension cells (CEM) were seeded into 96-well plates at a density of 5×10^3 cells per well and were treated with increasing concentrations of all halogenated analogs for 72 h. Measurement of cell proliferation was performed colorimetrically by 3-(4,5-dimethylthiazol-2-yl)-5-(3-carboxymethoxyphenyl)-2-(4-sulphophenyl)-2*H*-tetrazolium, inner salt (MTS) assay, using the CellTiter96 AQueous One Solution Reagent (Promega, Madison, WI). Cells were exposed to MTS for 3 h and absorbance was measured using a microplate reader (Molecular Devices, Sunnyvale, CA) at an optical density (OD) of 490 nm. The percentage of cell survival as a function of drug concentration for both the assays was then plotted to determine the IC_{50} value, which stands for the drug concentration needed to prevent cell proliferation by 50%.

2.7.3. 4′-6-Diamidino-2-phenylindole (DAPI) staining

Cell morphology was evaluated by fluorescence microscopy following DAPI staining (Vectashield, Vector Labs, Inc., Burlingame, CA). MDA-MB-231 cells were grown on poly-L-lysine coated coverslips in six-well plates and were treated with the halogenated analogs at 25 μM for 72 h. After incubation, coverslips were fixed in cold methanol and washed with PBS, stained with DAPI, and mounted on slides. Images were captured using a BX60 microscope (Olympus, Tokyo, Japan) with an 8-bit camera (Dage-MTI, Michigan City, IN) and IP Lab software (Scanalytics, Fairfax, VA). Apoptotic cells were identified by features characteristic of apoptosis (e.g. nuclear condensation, formation of membrane blebs and apoptotic bodies).

2.7.4. Tubulin-binding assay

Fluorescence titration for determining the tubulin-binding parameters was performed as described previously [29]. In brief, 9-F-nos, 9-Cl-nos, 9-Br-nos or 9-I-nos (0–100 μM) was incubated with 2 μM tubulin in 25 mM PIPES, pH 6.8, 3 mM $MgSO_4$, and 1 mM EGTA for 45 min at 37 °C. The relative intrinsic fluorescence intensity of tubulin was then monitored in a JASCO FP-6500 spectrofluorometer (JASCO, Tokyo, Japan) using a cuvette of 0.3-cm path length, and the excitation wavelength was 295 nm. The fluorescence emission intensity of noscapine and its derivatives at this excitation wavelength was negligible. A 0.3-cm path-length cuvette was used to minimize the inner filter effects caused by the absorbance of these agents at higher concentration ranges. In addition, the inner filter effects were corrected using a formula $F_{corrected} = F_{observed} \times \text{antilog}\,[(A_{ex} + A_{em})/2]$, where A_{ex} is the absorbance at the excitation wavelength and A_{em} is the absorbance at the emission wavelength. The dissociation constant (K_d) was determined by the formula: $1/B = K_d/[\text{free ligand}] + 1$, where B is the fractional occupancy and [free ligand] is the concentration of 9-F-nos, 9-Cl-nos, 9-Br-nos or 9-I-nos. The fractional

occupancy (B) was determined by the formula $B = \Delta F/\Delta F_{max}$, where ΔF is the change in fluorescence intensity when tubulin and its ligand are in equilibrium and ΔF_{max} is the value of maximum fluorescence change when tubulin is completely bound with its ligand. ΔF_{max} was calculated by plotting $1/\Delta F$ versus 1/[free ligand].

2.7.5. *Cell cycle analysis*

The flow cytometric evaluation of the cell cycle status was performed as described previously [12]. Briefly, 2×10^6 cells were centrifuged, washed twice with ice-cold PBS, and fixed in 70% ethanol. Tubes containing the cell pellets were stored at 4 °C for at least 24 h. Cells were then centrifuged at 1000 × *g* for 10 min and the supernatant was discarded. The pellets were washed twice with 5 ml of PBS and then stained with 0.5 ml of propidium iodide (0.1% in 0.6% Triton-X in PBS) and 0.5 ml of RNase A (2 mg/ml) for 45 min in dark. Samples were then analyzed on a FACSCalibur flow cytometer (Beckman Coulter Inc., Fullerton, CA).

2.7.6. *Immunofluorescence microscopy*

Cells adhered to poly-L-lysine coated coverslips were treated with noscapine and its halogenated analogs (9-F-nos, 9-Cl-nos, 9-Br-nos, 9-I-nos for 0, 12, 24, 48 and 72 h). After treatment, cells were fixed with cold (−20 °C) methanol for 5 min and then washed with phosphate-buffered saline (PBS) for 5 min. Non-specific sites were blocked by incubating with 100 μl of 2% BSA in PBS at 37 °C for 15 min. A mouse monoclonal antibody against α-tubulin (DM1A, Sigma) was diluted 1:500 in 2% BSA/PBS (100 μl) and incubated with the coverslips for 2 h at 37 °C. Cells were then washed with 2% BSA/PBS for 10 min at room temperature before incubating with a 1:200 dilution of a fluorescein-isothiocyanate (FITC)-labeled goat anti-mouse IgG antibody (Jackson ImmunoResearch, Inc., West Grove, PA) at 37 °C for 1 h. Coverslips were then rinsed with 2% BSA/PBS for 10 min and incubated with propidium iodide (0.5 μg/ml) for 15 min at room temperature before they were mounted with Aquamount (Lerner Laboratories, Pittsburgh, PA) containing 0.01% 1,4-diazobicyclo(2,2,2)octane (DABCO, Sigma). Cells were then examined using confocal microscopy for microtubule morphology and DNA fragmentation (at least 100 cells were examined per condition). Propidium iodide staining of the nuclei was used to visualize the multinucleated and micronucleated DNA in this study.

3. Results and discussion

Aromatic halogenation constitutes one of the most important reactions in organic synthesis. Although, bromine and chlorine are extensively used for carrying out electrophilic aromatic substitution reactions in the presence of their respective iron halides, their utility is limited because of the practical difficulty in handling of these reagents in laboratories compared to *N*-bromo- (NBS) and *N*-chlorosuccinimide (NCS). Thus, NBS and NCS have proven to be superior halogenating reagents provided benzylic halogenation is suppressed. For example, Schmid reported that benzene and toluene gave nuclear brominated derivatives in good yields with NBS and $AlCl_3$ without solvents under long reflux using a large amount of the catalyst (>1 equiv.) [30]. However, reactions using NBS in the presence of H_2SO_4, $FeCl_3$, and $ZnCl_2$ resulted in unsatisfactory yields (21–61%) together with the polysubstituted products. In another report by Lambert et al., aromatic substituted derivatives were obtained in good yields with NBS in 50% aqueous H_2SO_4 [31], however, this method required considerably high acidic conditions which are not suitable for acid labile compounds, such as noscapine. Thus, there still exists a need to develop selective, reproducible and efficient procedures for the halogenation of such labile aromatic compounds that eliminate the limitations associated with the above discussed synthetic methods and offer quantitative yields of the desired compounds. Our lead compound, noscapine consists of isoquinoline and benzofuranone ring systems joined by a labile C–C chiral bond and both these ring systems contain several vulnerable methoxy groups. Thus, achieving selective halogenation at C-9 position without disruption and cleavage of these labile groups and C–C bonds was challenging. After careful titration of many conditions, we have been successful in developing simple, selective, efficient, and reproducible synthetic procedures to achieve halogenation at C-9 position, that are discussed below.

First, we examined the bromination of noscapine with bromine water in the presence of HBr (Scheme 1). 9-Br-nos, (**2**) was prepared as described previously with minor modifications [12,32]. Noscapine (**1**) was dissolved in minimum amount of 48% hydrobromic acid with continuous stirring followed by the addition of freshly prepared bromine water over a period of 1 h until the appearance of an orange precipitate. The reaction mixture was then stirred at room temperature for 1 h

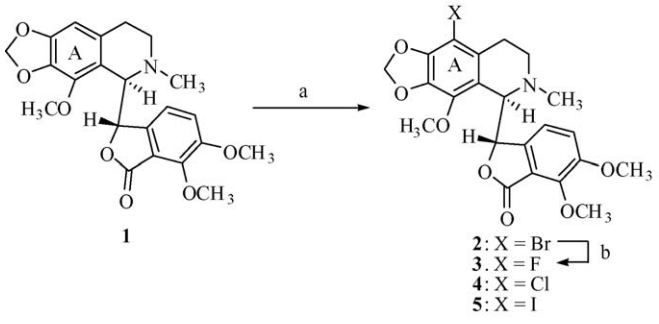

Scheme 1 – Semi-synthetic derivatives of noscapine. Reagents and reaction conditions—(a) compound *2*: Br_2-H_2O, 48% HBr, 82%; compound 4: SO_2Cl_2, $CHCl_3$, 90%; compound 5: Pyr-ICl, CH_3CN, 71%. (b) F_2, Amberlyst-A, THF, 74%.

to attain completion. Next, the resultant mixture was adjusted to pH 10 using ammonia solution to obtain 9-Br-nos (**2**) in 82% yield. Excess amount of HBr or longer reaction times were avoided because they resulted in the hydrolyzed products, meconine and cotarnine. The bromination took place selectively on ring A of isoquinoline nucleus at position C-9. An absence of C-9 aromatic proton at δ 6.30-ppm in the ^{1}H NMR spectrum of the product confirmed bromination at C-9 position. ^{13}C NMR and HRMS data support the structure of the compound.

Aromatic fluorination of noscapine was achieved by employing the fluoride form of Amberlyst-A 26, a macroreticular anion-exchange resin containing quaternary ammonium groups. The method described [33] for Hal/F exchange may also be applied to other Hal/Hal′ exchange reactions. In Br/F exchange reactions, good yields were obtained only when a large molar ratio of the resin with respect to the substrate was employed. Thus, after refluxing a solution of bromonoscapine in anhydrous THF and an excess of Amberlyst-A 26 (fluorine, polymer-supported, 10 mequiv. of dry resin; the average capacity of the resin is 4 mequiv./g) for 12 h, the resin was filtered off and the solvent was removed in vacuo to afford the desired compound (**3**) in 74% yield. The resin was recovered by washing with 1N NaOH and then rinsing thoroughly with water until neutrality to generate the hydroxy-form of the resin. It was then stirred overnight with 1N aqueous hydrofluoric acid, washed with acetone, ether and dried in a vacuum oven at 50 °C for 12 h to afford the regenerated Amberlyst-A 26 (fluorine, polymer-supported), which can be reused.

Next, we examined chlorination of noscapine using 1:1 equivalents of *N*-chlorosuccinimide in acetonitrile and ammonium nitrate or ferric chloride as catalyst [34]. However, this method did not provide satisfactory yields. Chlorination of noscapine using sulfuryl chloride in chloroform at low temperature gave excellent yields and the desired regioselectivity. Using this method, 9-Cl-nos (**4**) was obtained in 90% yield (Scheme 1) [35]. The chlorination took place chemoselectively on ring A of isoquinoline nucleus at position C-9. An absence of C-9 aromatic proton at δ 6.30-ppm in the ^{1}H NMR spectrum of the product confirmed chlorination at C-9 position. ^{13}C NMR and HRMS data support the structure of the compound.

Since iodine is the least reactive halogen towards electrophilic substitution, direct iodination of aromatic compounds with iodine presents difficulty and requires strong oxidizing conditions. Thus, a large diversity of methods for synthesis of aromatic iodides have been reported [36]. Some of these reported procedures involved harsh conditions such as nitric acid–sulfuric acid system (HNO_3/H_2SO_4), iodic acid (HIO_3) or periodic acid (HIO_4/H_2SO_4), potassium permanganate–sulfuric acid system ($KMnO_4/H_2SO_4$), chromia (CrO_3) in acidic solution with iodine, vanadium salts/triflic acid at 100 °C, and lead acetate–acetic acid system [$Pb(OAc)_4$/HOAc]. *N*-Iodosuccinimide and triflic acid (NIS/CF_3SO_3H) has also been reported for the direct iodination of highly deactivated aromatics. In addition, iodine–mercury(II) halide (I_2/HgX_2), iodine monochloride/silver sulfate/sulfuric acid system ($ICl/Ag_2SO_4/H_2SO_4$), *N*-iodosuccinimide/trifluoroacetic acid (NIS/CF_3CO_2H), iodine/silver sulfate (I_2/Ag_2SO_4), iodine/1-fluoro-4-chloromethyl-1,4-diazoniabicyclo[2.2.2]octane bis(tetrafluoroborate) (I_2/F-TEDA-BF_4), *N*-iodosuccinimide/acetonitrile (NIS/CH_3CN), and ferric nitrate/nitrogen tetroxide [$Fe(NO_3)_3/N_2O_4$] are also routinely employed for iodination. Nonetheless, iodination of noscapine even under the most gentle conditions gave only the hydrolysis products, meconine and cotarnine [37]. In addition, direct aromatic iodination of noscapine using thallium trifluoroacetate or iodine monochloride also resulted in bond fission between C-5 and C-3′ under acidic conditions. Thus, we tried different reaction conditions based upon varying pH, and found that successful introduction of the iodine atom at the desired C-9 position without disrupting other groups and bonds was stringently dependent on the acidity of the reaction media. A low acidic environment was conducive to effect iodination, whereas, higher acidity was detrimental to the iodination reaction. Thus, in this present work, we used two different complexes of iodine chloride for iodination: pyridine–iodine chloride and potassium iododichloride. Although the reaction with potassium iododichloride gave 9-I-nos (**5**), the yield was low and the desired product was associated with the undesirable hydrolyzed products. A suggestive reason for hydrolysis reaction could be the generation of excess amount of conc. hydrochloric acid in the reagent mixture. Since it was necessary to avoid excess acidity, we then employed excess amounts of potassium chloride. Although potassium iododichloride solutions are most conveniently prepared by the addition of commercial iodine chloride to a solution of potassium chloride, it was possible to modify the procedure of Gleu and Jagemann, wherein, an iodide solution was oxidized with the calculated quantity of iodate in the presence of excess potassium chloride [38]. The pyridine–iodine chloride complex was prepared directly from pyridine and potassium iododichloride and this procedure avoided the separate isolation of the pyridine–iodine chloride–hydrogen chloride complex [39]. Thus, 9-I-nos (**5**) was prepared by treating a solution of noscapine in acetonitrile with pyridine–iodine chloride at room temperature for 6 h followed by raising the temperature to 100 °C for another 6 h. After cooling, excess ammonia was added and filtered through a celite pad to remove the black nitrogen triiodide. The filtrate was made acidic with 1 M HCl and filtered to collect the yellow solid, washed with water and air-dried to obtain the desired compound in 76% yield. A valuable advantage of this procedure lies in its applicability for the regioselective aromatic iodination of complex natural products.

3.1. *Halogenated noscapine analogs have higher tubulin-binding activity than noscapine*

We first asked if all of our halogenated analogs bind tubulin like the parent compound, noscapine. Tubulin, like many other proteins, contains fluorescent amino acids like tryptophans and tyrosines and the intensity of the fluorescence emission is dependent upon the micro-environment around these amino acids in the folded protein. Agents that bind tubulin typically change the micro-environment and the fluorescent properties of the target protein [18,40,41]. Measuring these fluorescent changes has become a standard method for determining the binding properties of tubulin ligands including the classical compound colchicine [42]. We thus

employed this standard method to determine the dissociation constant (K_d) between tubulin and the halogenated analogs (9-F-nos, 9-Cl-nos, 9-Br-nos, and 9-I-nos). We found that all halogenated noscapine analogs quenched tubulin fluorescence in a concentration-dependent manner (Fig. 1A, upper panels). We have previously reported the dissociation constant (K_d) of 144 ± 2.8 μM for noscapine binding to tubulin [18], 54 ± 9.1 μM for 9-Br-nos [12] binding to tubulin and 40 ± 8μM for 9-Cl-nos [43] binding to tubulin. The double reciprocal plots yielded a dissociation constant (K_d) of 81 ± 8 μM for 9-F-nos, and 22 ± 4μM for 5-I-nos, binding to tubulin. These results thus indicate that all halogenated analogs bind to tubulin with a greater affinity than noscapine in the following order of magnitude: 9-I-nos > 9-Cl-nos > 9-Br-nos > 9-F-nos > Nos.

3.2. *Effects of halogenated noscapine analogs on proliferation of cancer cells*

Having identified tubulin as the target molecule, we extended our pharmacological study at the cellular level to determine if all the halogenated analogs affected cancer cell proliferation. As a preliminary screen, all compounds including the parent noscapine were evaluated for their antiproliferative activity in three human cancer cell lines; human breast adenocarcinoma cells (estrogen- and progesterone-receptor positive, MCF-7 and estrogen- and progesterone-receptor negative, MDA-MB-231) and human lymphoblastoid cells CEM. The test compounds were dissolved in DMSO to provide a concentration range of 10 nm–1000 μM. We used the Sulforhodamine B (SRB) in vitro proliferation assay to determine the IC_{50} values that stand for the drug concentration required to achieve a cell kill of 50%. The IC_{50} values for all the halogenated analogs for these three cell lines are collated in Table 2. 9-I-nos was found to possess modest cytotoxic effects and in sharp contrast, 9-F-nos, 9-Cl-nos and 9-Br-nos exhibited potent cytotoxic activity. The IC_{50} value amounted to 1.9 ± 0.3 and 1.0 ± 0.2 μM with 9-Cl-nos and 9-Br-nos, respectively, for MCF-7 cells, which reflects a pronounced antiproliferative activity. Surprisingly, 9-Br-nos showed a ~40-fold higher cytotoxic activity (IC_{50} = 1.0 ± 0.2 μM) than noscapine (IC_{50} = 39.6 ± 2.2 μM). Parenthetically, it is worth mentioning that a similar low IC_{50} value of 1.2 ± 0.3 and 1.9 ± 0.2 μM was measured using 9-Cl-nos and 9-Br-nos, respectively, for the CEM cells. Interestingly, the IC_{50} values of 1.9 ± 0.3 and 3.5 ± 0.4 μM with 9-Cl-nos for MDA-MB-231 and MCF-7 cells, respectively, are close suggesting that 9-Cl-nos inhibits cellular proliferation of cancer cells independent of hormone receptor status. Thus this preliminary screen with the three chosen cell lines revealed 9-F-nos, 9-Cl-nos, 9-Br-nos as potent cytotoxic compounds exemplified by their much lower IC_{50} values as compared to noscapine. The iodo-substituent at position-9 resulted in improved cytotoxic activity than the parent noscapine in some cell types, such as MDA-MB-231, but not better than noscapine in other cell types, such as CEM.

Although a definitive correlation of the sensitivity of cancer cells to these analogs cannot yet be established at this stage, it is evident that tubulin represents a potential target for these compounds. Our results suggest that the IC_{50} values do not show a correlation among these analogs and are cell-type dependent. The three analogs (9-F-nos, 9-Cl-nos and 9-Br-nos) have been submitted by our laboratory for testing by the National Cancer Institute (NCI), through its Developmental Therapeutics Program (DTP), against their panel of 60 human cancer cell lines. We have so far received the results of 9-Br-nos, which are presented in Fig. 2. The panel of 60 human tumor cell lines is organized into subpanels representing

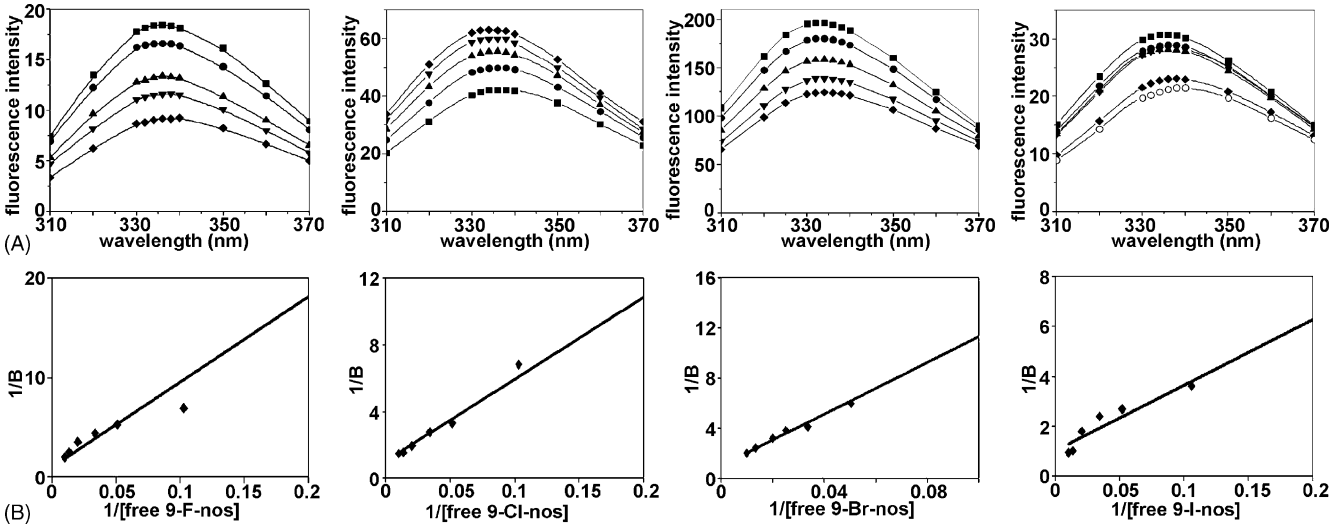

Fig. 1 – Fluorescence quenching of tubulin by halogenated derivatives of noscapine namely, 9-F-nos, 9-Cl-nos, 9-Br-nos and 9-I-nos. (A) The tubulin fluorescence emission spectrum is quenched by 9-F-nos [control (■), 25 μM (●), 50 μM (▲), 75 μM (▼), and 100 μM (◆)], 9-Cl-nos [control (◆), 25 μM (▼), 50 μM (▲), 75 μM (●), and 100 μM (■)], 9-Br-nos [control (■), 25 μM (●), 50 μM (▲), 75 μM (▼), and 100 μM (◆)] and 9-I-nos [control (■), 25 μM (▼), 50 μM (▲), 75 μM (◆), and 100 μM (○)] in a concentration-dependent manner. (B) Double reciprocal plots showing a dissociation constant (K_d) of 81 ± 8 for 9-F-nos binding to tubulin, 40 ± 8 μM for 9-Cl-nos, 54 ± 9.1 μM for 9-Br-nos and 22 ± 4 μM for 9-I-nos. Values are mean ± S.D. for four experiments performed in triplicate ($p < 0.05$). The graphs shown are a representative of four experiments performed.

Table 2 – IC_{50} values of halogenated derivatives of noscapine

	IC_{50} (μM)				
	Nos	9-F-nos	9-Cl-nos	9-Br-nos	9-I-nos
MCF-7	39.6 ± 2.2	3.3 ± 0.8	1.9 ± 0.3	1.0 ± 0.2	45.6 ± 3.1
MDA-MB-231	36.3 ± 1.8	8.2 ± 0.6	3.5 ± 0.4	3.3 ± 0.4	25.6 ± 2.4
CEM	16.6 ± 2.4	2.3 ± 0.7	1.2 ± 0.3	1.9 ± 0.2	38.9 ± 3.5

Values represent mean ± S.D. for three independent experiments performed in triplicate.

leukemia, non-small cell lung, colon, central nervous system (CNS), melanoma, renal, ovarian, breast and prostrate cancer lines. Fig. 2 shows a bar-graphical representation depicting a comparison of the IC_{50} values of both noscapine and 9-Br-nos for the NCI 60 tumor cell line panel.

Besides the antiproliferative effect, morphological evaluation using DAPI staining revealed condensed chromatin along with numerous fragmented nuclei (shown by white arrowheads), indicative of apoptotic cell death (Fig. 3) that was investigated next.

3.3. *Halogenated noscapine analogs alter the cell cycle profile and cause mitotic arrest at G_2/M phase more actively than noscapine*

To investigate the precise mechanisms of cell death, we next examined the effect of halogenated analogs on percent G_2/M cells (mitotic index) and percent sub-G_1 cells (apoptotic index) as a function of dose and time in MCF-7 cells using fluorescence activated cell sorting (FACS) analysis. We studied the effect of all compounds including noscapine at three doses—5, 10 and

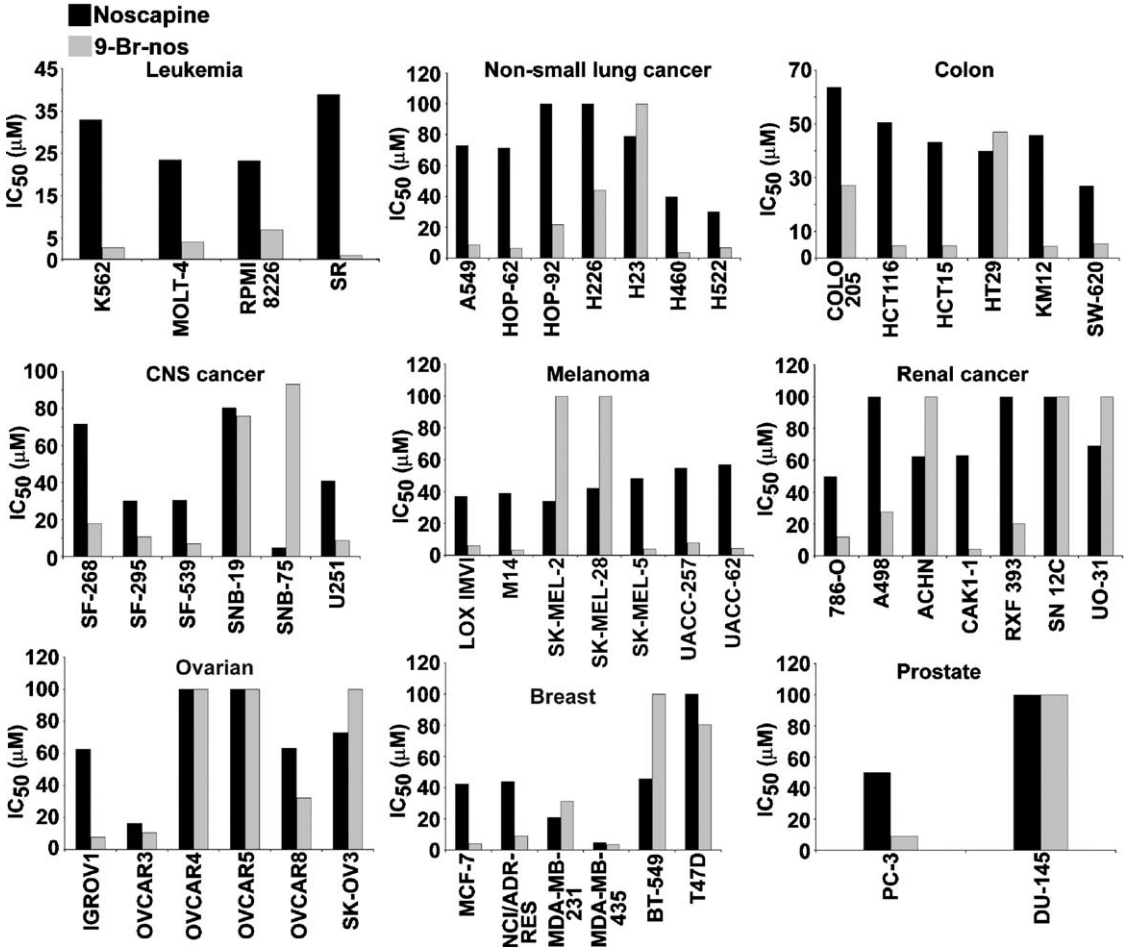

Fig. 2 – 9-Br-nos is much more active than noscapine in inhibiting the proliferation of various human cancer cells. The panel of 60 human tumor cell lines is organized into subpanels representing leukemia, non-small cell lung, colon, CNS, melanoma, renal, ovarian, breast and prostrate cancer lines. Cells were treated with noscapine and 9-Br-nos at increasing gradient concentrations for 48 h. The IC_{50} values, which stand for the drug concentration needed to prevent cell proliferation by 50% was then measured using an in vitro Sulforhodamine B assay. Panels show bar-graphically the comparison of IC_{50} values of noscapine (black bars) and 9-Br-nos (grey bars) for cancer cell lines of various tissue origins.

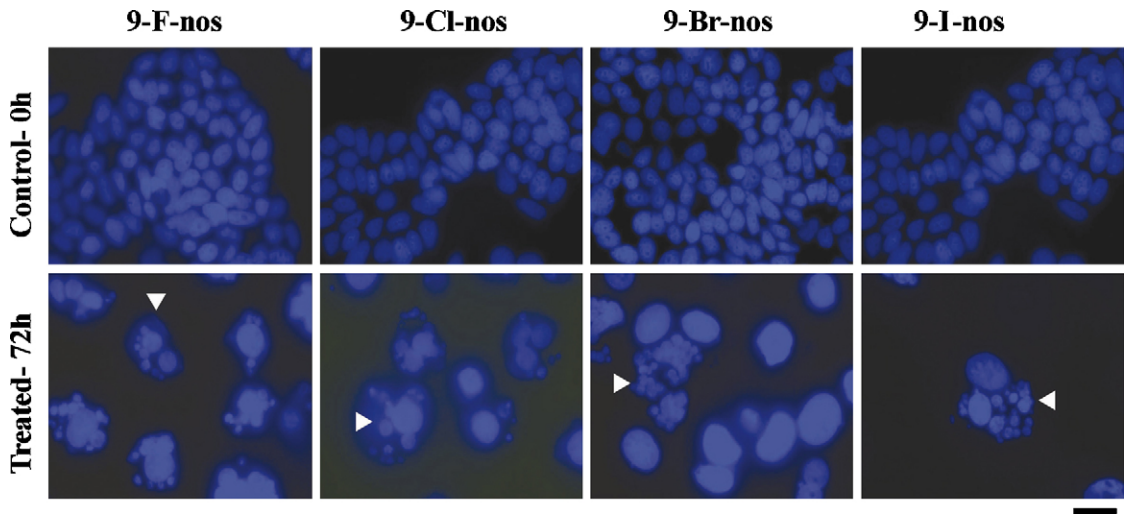

Fig. 3 – Morphologic criteria for apoptotic cell death include, for example, chromatin condensation with aggregation along the nuclear envelope and plasma membrane blebbing followed by separation into small, apoptotic bodies. Panels show morphological evaluation of nuclei stained with DAPI from control cells (upper panels) and cells treated with 25 μM concentration of 9-F-nos, 9-Cl-nos, 9-Br-nos, and 9-I-nos for 72 h (lower panels) using fluorescence microscopy. Several typical features of apoptotic cells such as condensed chromosomes, numerous fragmented micronuclei, and apoptotic bodies are evident (indicated by white arrowheads) upon 72 h of drug treatment (scale bar = 15 μm).

25 μM for 0, 24, 48 and 72 h of drug treatment. Fig. 4 (Panels A–F) shows the cell cycle profile in a three-dimensional disposition for all the compounds included in the course of this study. Fluorescently labeled DNA is a good indicator of cell cycle progression and cell death. An unreplicated complement of diploid (2N) DNA cells represents the G_1 phase while duplicated tetraploid (4N) DNA cells represent G_2 and M phases. Cells in the process of DNA duplication between diploid and tetraploid

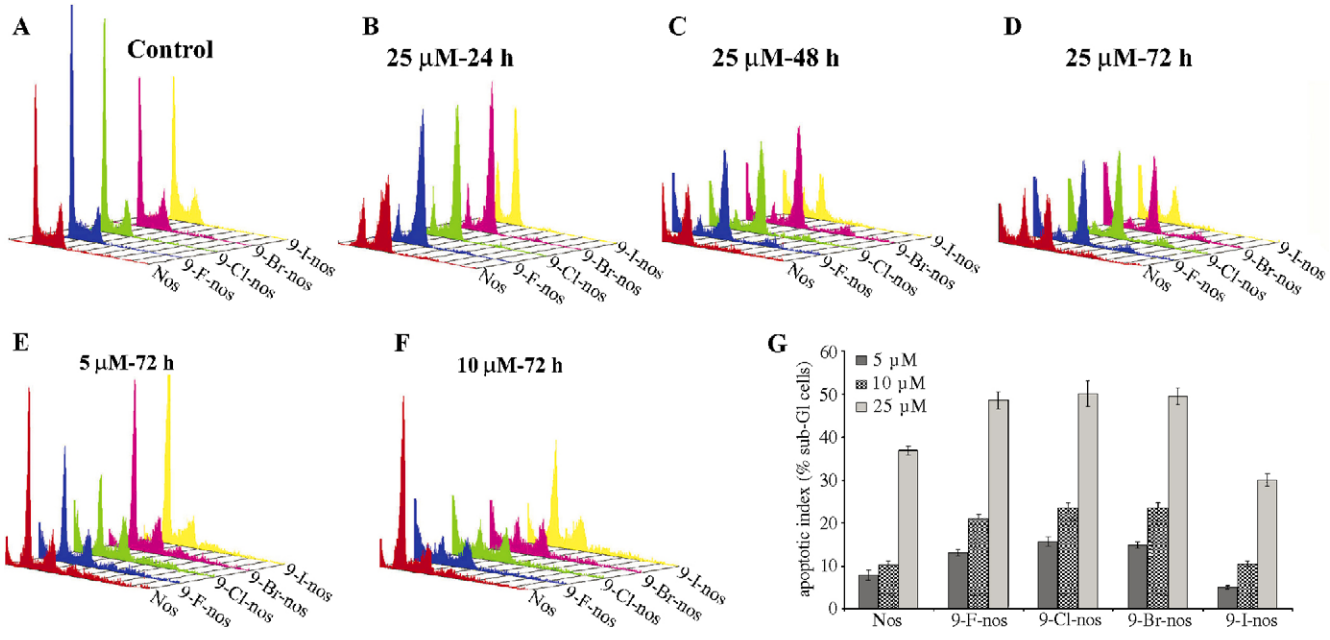

Fig. 4 – Noscapine and its halogenated analogs inhibit cell cycle progression at mitosis followed by the appearance of a characteristic hypodiploid (sub-G_1) DNA peak, indicative of apoptosis. Panels A–D depict analyses of cell cycle distribution in a three-dimensional disposition as determined by flow cytometry in MCF-7 cells treated with 25 μM concentration of all five compounds (Nos, 9-F-nos, 9-Cl-nos, 9-Br-nos and 9-I-nos) for 0, 24, 48 and 72 h, respectively. Panels E and F show similar three-dimensional profiles for MCF-7 cells treated for 72 h with 5 and 10 μM concentration of each compound to evaluate the differences in percent sub-G_1 population among the five compounds. Panel G is a graphical representation of the quantitation of apoptotic index (percent sub-G_1 cells) at the three dose regimes (5, 10 and 25 μM) at 72 h for all compounds. Values and error bars shown in the graph represent the means and standard deviations, respectively, of three independent experiments performed in triplicate.

peaks represent S phase when DNA is being synthesized. Less than diploid DNA appears in populations of dying cells that degrade their DNA to different extents. Treatment of MCF-7 cells with these compounds for 0, 24, 48 and 72 h led to profound perturbations of the cell cycle profile at 25 μM (Fig. 4, Panels A–D). Our results show that 9-F-nos, 9-Cl-nos and 9-Br-nos induced a massive accumulation of cells in the G_2/M phase at 24 h. For example, the G_2/M cell population increased from 18.5% in the control to ~66% in MCF-7 cells treated with 25 μM 9-F-nos for 24 h. The distribution of cell population over G_0/G_1, S, G_2/M and sub-G_1 phases of the cell cycle for 25 μM concentration is shown in Table 3. More subtle effects that helped us to determine the sensitivity of MCF-7 cells to halogenated analogs for induction of mitotic block were evident at lower dose regimes, i.e. 5 and 10 μM. Panels E and F (Fig. 4) show the three-dimensional cell cycle profile of MCF-7 cells treated for 72 h with 5 and 10 μM, respectively, for all the five compounds. In parallel to the G_2/M block, a characteristic hypodiploid DNA content peak (sub-G_1) is seen to be rising at 48 and 72 h of drug treatment for all the three doses studied. The progressive generation of cells having hypodiploid DNA content indicates apoptotic cells with fragmented DNA. The percent sub-G_1 population for the three doses (5, 10 and 25 μM) has been plotted for all the compounds in Fig. 4, Panel G. It is evident from the bar-graphical representation that a 72 h treatment at 25 μM for MCF-7 cells, the percentage of sub-G_1 cells is almost similar for 9-F-nos, 9-Cl-nos and 9-Br-nos. However, the sub-G_1 population is slightly lower for 9-I-nos than noscapine at 25μM. At lower doses, the percent sub-G_1 cells were higher for 9-F-nos, 9-Cl-nos and 9-Br-nos than the parent compound noscapine. Thus, we can clearly see differences at 5 and 10 μM concentrations of the halogenated compounds in the extent of their deleterious effect on the cell cycle by an increase in the percentage of sub-G_1 cells having hypodiploid DNA content, characteristic of apoptosis.

3.4. *Effect of halogenated noscapine analogs on spindle architecture and nuclear morphology*

To test whether these halogenated noscapine analogs induce spindle abnormalities prior to apoptotic cell death indicated by nuclear fragmentation of dying cells, we examined the spindle architecture and nuclear morphology of MCF-7 cells treated with the halogenated analogs using confocal microscopy (Fig. 5). MCF-7 cells were treated with 25 μM 9-F-nos, 9-Cl-nos, 9-Br-nos and 9-I-nos for 0, 12, 24, 48 and 72 h. We found that while untreated MCF-7 cells exhibited normal radial microtubule arrays in normal interphase cells, treated cells exhibited pronounced spindles and condensed chromosomes that are not organized at the metaphase plate indicating mitotic arrest commencing as early as 12 h, and maximizing at 24 h of drug treatment, when numerous mitotically arrested cells were visible (indicated by white arrowheads, Fig. 5). This was probably due to the activation of the spindle assembly checkpoint, a cellular surveillance mechanism that monitors the integrity of the mitotic spindle [20]. After 48 h of treatment, the population of arrested cells decreased and we could observe micronucleated and multinucleated cells (white arrowheads, Fig. 5, 9-Br-nos, 48 h). Our immunofluorescence experiments correlated well with our cell cycle progression experiments that offered comparable results at similar time

Table 3 – Effect of halogenated derivatives of noscapine on cell cycle progression of MCF-7 cells

Cell cycle parameters (%)	0 h				24 h				48 h				72 h			
	Sub-G_1	G_0/G_1	S	G_2/M	Sub-G_1	G_0/G_1	S	G_2/M	Sub-G_1	G_0/G_1	S	G_2/M	Sub-G_1	G_0/G_1	S	G_2/M
Nos	0.2 ± 0.03	54.8 ± 3.2	13.2 ± 0.2	29.9 ± 2.2	10.2 ± 1.2	18.3 ± 3.3	3.4 ± 0.8	50.2 ± 3.6	36.8 ± 3.7	19.8 ± 1.9	4.1 ± 0.6	28.07 ± 0.2	36.9 ± 0.2	20.5 ± 0.2	7.06 ± 0.2	26.3 ± 0.2
9-F-nos	0.2 ± 0.04	67.7 ± 5.6	11.9 ± 1.5	18.5 ± 2.2	6.8 ± 2.1	10.8 ± 2.4	3.8 ± 1.1	65.9 ± 4.4	34.5 ± 2.5	7.9 ± 2.8	3.5 ± 0.8	43.7 ± 2.9	48.6 ± 3.3	5.2 ± 2.2	3.6 ± 1.5	34.4 ± 3.4
9-Cl-nos	1.4 ± 0.5	69 ± 5.6	7.5 ± 1.6	20.7 ± 3.4	15.3 ± 2.5	11.5 ± 2.7	4.3 ± 1.4	59.7 ± 5.2	38.1 ± 3.2	8 ± 3.3	4 ± 1.1	42.4 ± 3.8	50.2 ± 2.5	5.9 ± 1.9	4.1 ± 1.4	35.3 ± 3.9
9-Br-nos	0.2 ± 0.1	53.3 ± 2.8	12.7 ± 1.8	28.9 ± 4.4	6.9 ± 2.4	10.4 ± 1.8	3.4 ± 1.2	61.9 ± 3.6	35.1 ± 3.5	6.5 ± 2.5	2.8 ± 0.7	43.8 ± 3.4	49.6 ± 2.7	4.6 ± 2.1	2.4 ± 1.6	33.7 ± 3.5
9-I-nos	0.3 ± 0.2	60.6 ± 4.6	13.9 ± 2.3	23.1 ± 3.7	7.7 ± 1.7	17 ± 2.3	3.1 ± 1.3	44.5 ± 5.1	28.1 ± 3.1	15.4 ± 4.5	2.9 ± 0.6	25.9 ± 4.1	30.1 ± 3.1	17 ± 1.9	4.9 ± 2.2	20.7 ± 2.2

MCF-7 cells were treated with 25 μM solution for the indicated time (h) before being stained with propidium iodide (PI) for cell cycle analysis. Values represent mean ± S.E.M.

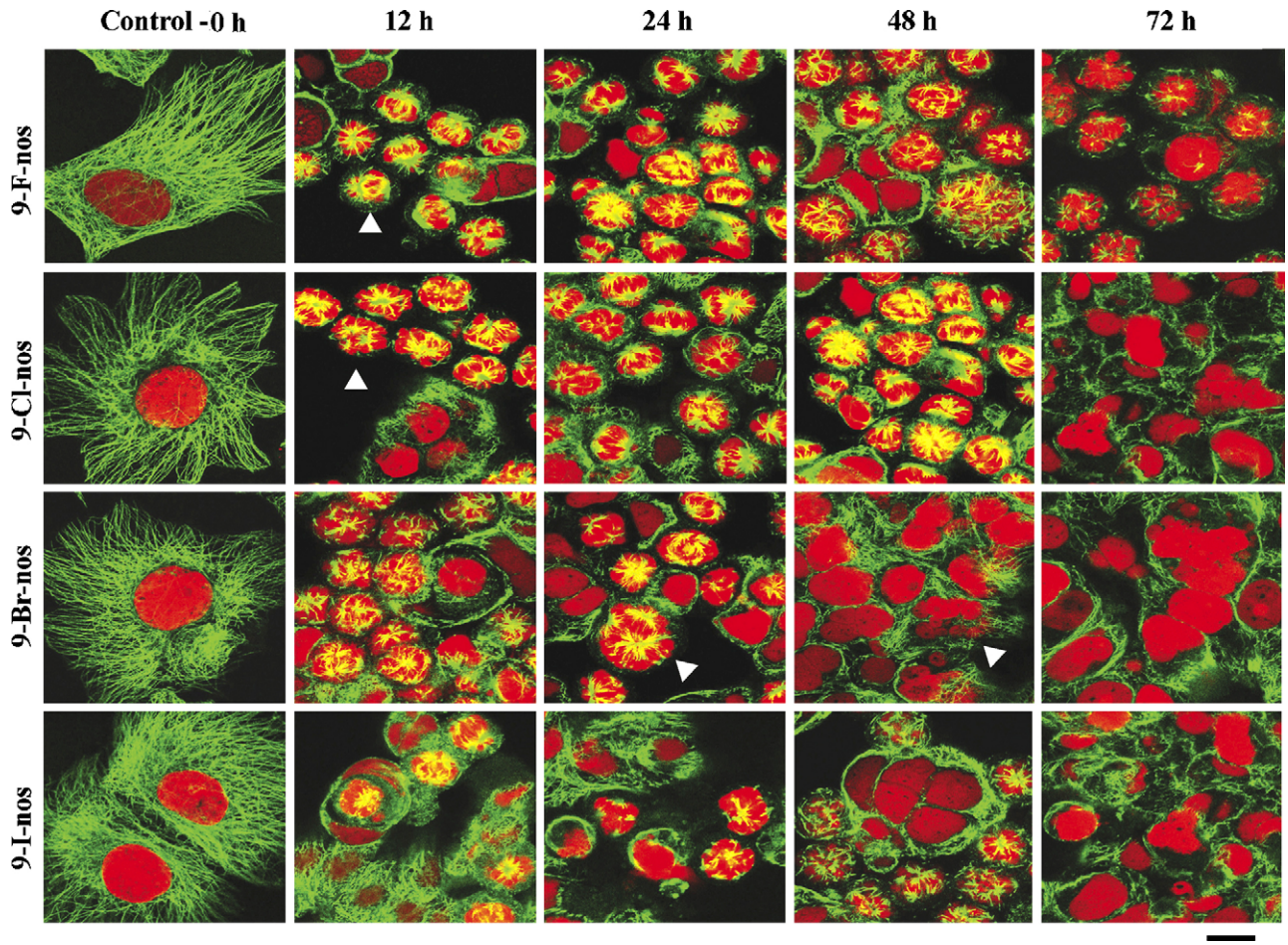

Fig. 5 – Halogenated noscapine analogs induce spindle abnormalities. Panels show immunofluorescence confocal micrographs of MCF-7 cells treated for 0, 12, 24, 48 and 72 h with 25 μM concentration of all five compounds (Nos, 9-F-nos, 9-Cl-nos, 9-Br-nos and 9-I-nos). As expected, mitotic figures are abundant at 24 h while apoptotic figures start to appear at 48 h (scale bar = 30 μm).

regimens and displayed DNA degradation (sub-G_1 population) at 48 and 72 h of treatment.

4. Conclusion

In summary, we have provided simplest methods for the direct, and regioselective halogenation of noscapine that provide halogenated products in high quantitative yields. Although a plethora of reagents and reaction conditions have been reported for aromatic halogenation, most of them did not work for noscapine that is readily hydrolysable. We provide synthetic strategies that effect the desired transformations under mild conditions. Most importantly, our results show that halogenation of noscapine increases its tubulin-binding activity and impacts its therapeutic potential for a variety of cancer cell types. Furthermore, the mechanism of apoptotic cell death caused by these halogenated analogs is preserved, in that, like noscapine, cell death is preceded by extensive mitotic arrest. Taken together, like noscapine, these analogs indicate a great potential for further preclinical and clinical evaluation.

Acknowledgements

We wish to thank Dr. William Beck for providing CEM cells used in this study. We are grateful to Dr. Wu and Dr. Fred Strobel of Department of Chemistry, Emory University for assistance with the NMR and High Resolution Mass spectrometry, respectively.

REFERENCES

[1] Mitchison TJ, Kirschner M. Dynamic instability of microtubule growth. Nature 1984;312:237–42.
[2] Kirschner M, Mitchison TJ. Beyond self-assembly: from microtubules to morphogenesis. Cell 1986;45:329–42.
[3] McIntosh JR. The role of microtubules in chromosome movement. In: Hyams JS, Lloyd CW, editors. Microtubules. New York: Wiley-Liss; 1994. p. 413–34.
[4] Jordan MA, Wilson L. Microtubules as a target for anticancer drugs. Nat Rev Cancer 2004;4:253–65.
[5] Zhou J, Giannakakou P. Targeting microtubules for cancer chemotherapy. Curr Med Chem Anticancer Agents 2005;5:65–71.

[6] van Tellingen O, Sips JH, Beijnen JH, Bult A, Nooijen WJ. Pharmacology, bio-analysis and pharmacokinetics of the vinca alkaloids and semi-synthetic derivatives. Anticancer Res 1992;12:1699–715.
[7] Rowinsky EK. The development and clinical utility of the taxane class of antimicrotubule chemotherapy agents. Annu Rev Med 1997;48:353–74.
[8] Crown J, O'Leary M. The taxanes: an update. Lancet 2000;355:1176–8.
[9] Anderson JT, Ting AE, Boozer S, Brunden KR, Crumrine C, Danzig J, et al. Identification of novel and improved antimitotic agents derived from noscapine. J Med Chem 2005;48:7096–8.
[10] Anderson JT, Ting AE, Boozer S, Brunden KR, Danzig J, Dent T, et al. Discovery of S-phase arresting agents derived from noscapine. J Med Chem 2005;48:2756–8.
[11] Aneja R, Zhou J, Vangapandu SN, Zhou B, Chandra R, Joshi HC. Drug-resistant T-lymphoid tumors undergo apoptosis selectively in response to an antimicrotubule agent, EM011. Blood 2006;107:2486–92.
[12] Zhou J, Gupta K, Aggarwal S, Aneja R, Chandra R, Panda D, et al. Brominated derivatives of noscapine are potent microtubule-interfering agents that perturb mitosis and inhibit cell proliferation. Mol Pharmacol 2003;63:799–807.
[13] Zhou J, Liu M, Aneja R, Chandra R, Joshi HC. Enhancement of paclitaxel-induced microtubule stabilization, mitotic arrest, and apoptosis by the microtubule-targeting agent EM012. Biochem Pharmacol 2004;68:2435–41.
[14] Zhou J, Liu M, Luthra R, Jones J, Aneja R, Chandra R, et al. EM012, a microtubule-interfering agent, inhibits the progression of multidrug-resistant human ovarian cancer both in cultured cells and in athymic nude mice. Cancer Chemother Pharmacol 2005;55:461–5.
[15] Checchi PM, Nettles JH, Zhou J, Snyder JP, Joshi HC. Microtubule-interacting drugs for cancer treatment. Trends Pharmacol Sci 2003;24:361–5.
[16] Joshi HC, Zhou J. Noscapine and analogues as potential chemotherapeutic agents. Drug News Perspect 2000;13:543–6.
[17] Seetharaman J, Rajan SS. Crystal and molecular structure of noscapine. Zeftschrm fur Kristamographic 1995;210:111–3.
[18] Ye K, Ke Y, Keshava N, Shanks J, Kapp JA, Tekmal RR, et al. Opium alkaloid noscapine is an antitumor agent that arrests metaphase and induces apoptosis in dividing cells. Proc Natl Acad Sci USA 1998;95:1601–6.
[19] Ye K, Zhou J, Landen JW, Bradbury EM, Joshi HC. Sustained activation of p34(cdc2) is required for noscapine-induced apoptosis. J Biol Chem 2001;276:46697–700.
[20] Zhou J, Panda D, Landen JW, Wilson L, Joshi HC. Minor alteration of microtubule dynamics causes loss of tension across kinetochore pairs and activates the spindle checkpoint. J Biol Chem 2002;277:17200–8.
[21] Zhou J, Gupta K, Yao J, Ye K, Panda D, Giannakakou P, et al. Paclitaxel-resistant human ovarian cancer cells undergo c-Jun NH_2-terminal kinase-mediated apoptosis in response to noscapine. J Biol Chem 2002;277:39777–85.
[22] Ke Y, Ye K, Grossniklaus HE, Archer DR, Joshi HC, Kapp JA. Noscapine inhibits tumor growth with little toxicity to normal tissues or inhibition of immune responses. Cancer Immunol Immunother 2000;49:217–25.
[23] Landen JW, Lang R, McMahon SJ, Rusan NM, Yvon AM, Adams AW, et al. Noscapine alters microtubule dynamics in living cells and inhibits the progression of melanoma. Cancer Res 2002;62:4109–14.
[24] Landen JW, Hau V, Wang MS, Davis T, Ciliax B, Wainer BH, et al. Noscapine crosses the blood–brain barrier and inhibits glioblastoma growth. Clin Cancer Res 2004;10:5187–201.
[25] Dahlstrom B, Mellstrand T, Lofdahl C, Johansson M. Pharmacokinetic properties of noscapine. Eur J Clin Pharmacol 1982;22:535–9.
[26] Segal MS, Goldstein MM, Attinger EO. The use of noscapine (Narcotine) as an antitussive agent. Dis Chest 1957;32:305–9.
[27] Loder RE. Safe reduction of the cough reflex with noscapine: a preliminary communication on a new use for an old drug. Anaesthesia 1969;24:355–8.
[28] Skehan P, Storeng R, Scudiero D, Monks A, McMahon J, Vistica D, et al. New colorimetric cytotoxicity assay for anticancer-drug screening. J Natl Cancer Inst 1990;82: 1107–12.
[29] Joshi HC, Zhou J. Gamma tubulin and microtubule nucleation in mammalian cells. Methods Cell Biol 2001;67:179–93.
[30] Schmid H. Bromination with bromosuccinimide in the presence of catalysts. II. Helv Chim Acta 1946;29:1144–51.
[31] Lambert FL, Ellis WD, Parry RJ. Halogenation of aromatic compounds by *N*-bromo- and *N*-chlorosuccinimide under ionic conditions. J Org Chem 1965;30:304–6.
[32] Dey BB, Srinivasan TK. Cotarnine series. IV. 5-Bromonarcotine, 5-bromocotarnine, 5-bromohydrocotarnine and 5-bromonarceine and their derivatives. J Indian Chem Soc 1935;12:526–36.
[33] Cainelli G, Manescalchi F. Polymer-supported reagents. The use of anion-exchange resins in the synthesis of primary and secondary alkyl fluorides from alkyl halides or alkyl methanesulfonates. Synthesis 1976;472–3.
[34] Tanemura K, Suzuki T, Nishida Y, Satsumabayashi K, Horaguchi T. Halogenation of aromatic compounds by *N*-chloro-, *N*-bromo- and *N*-iodosuccinimide. Chem Lett 2003;32:932–3.
[35] Stokker GE, Deana AA, deSolms SJ, Schultz EM, Smith RL, Cragoe Jr EJ, et al. 2-(Aminomethyl)phenols, a new class of saluretic agents. 1. Effects of nuclear substitution. J Med Chem 1980;23:1414–27.
[36] Hajipour AR, Arbabian M, Ruoho AE. Tetramethylammonium dichloroiodate: an efficient and environmentally friendly iodination reagent for iodination of aromatic compounds under mild and solvent-free conditions. J Org Chem 2002;67:8622–4.
[37] Lee DU. (−)-β-Narcotine: a facile synthesis and the degradation with ethyl chloroformate. Bull Korean Chem Soc 2002;23:1548–52.
[38] Gleu K, Jagemann W. Action of iodine monochloride upon heterocyclic bases. J Prakt Chem 1936;145:257–64.
[39] Firouzabadi H, Iranpoor N, Shiri M. Direct and regioselective iodination and bromination of benzene naphthalene and other activated aromatic compounds using iodine and bromine or their sodium salts in the presence of the $Fe(NO_3)_3$. 1. $5N_2O_4$/charcoal system. Tetrahedron Lett 2003;44:8781–5.
[40] Peyrot V, Leynadier D, Sarrazin M, Briand C, Menendez M, Laynez J, et al. Mechanism of binding of the new antimitotic drug MDL 27048 to the colchicine site of tubulin: equilibrium studies. Biochemistry 1992;31:11125–32.
[41] Panda D, Singh JP, Wilson L. Suppression of microtubule dynamics by LY290181. J Biol Chem 1997;272:7681–7.
[42] Andreu JM, Gorbunoff MJ, Medrano FJ, Rossi M, Timasheff SN. Mechanism of colchicine binding to tubulin. Tolerance of substituents in ring C′ of biphenyl analogues. Biochemistry 1991;30:3777–86.
[43] Aneja R, Lopus M, Zhou J, Vangapandu SN, Ghaleb A, Yao J, Nettles JH, Zhou B, Gupta M, Panda D, Chandra R, Joshi HC. Rational design of the microtubule-targeting anti-breast cancer drug EM015. Cancer Res 2006;66: 3782–91.